



Imaging the membrane lytic activity of bioactive peptide laticin 2a

Amy Won, Annamaria Ruscito, Anatoli Ianoul*

Department of Chemistry, Carleton University, Ottawa, Ontario, Canada

ARTICLE INFO

Article history:

Received 1 June 2012

Received in revised form 25 July 2012

Accepted 30 July 2012

Available online 3 August 2012

Keywords:

Supported lipid bilayer

Lipid raft

Line tension

Membrane thinning

Interdigitation

Peptide oligomerization

ABSTRACT

Laticin 2a (ltc2a, GLFGKLIKFKGRKAISYAVKKARGKH-COOH) is a short linear antimicrobial and cytolytic peptide extracted from the venom of the Central Asian spider, *Lachesana tarabaevi*, with lytic activity against Gram-positive and Gram-negative bacteria, erythrocytes, and yeast at micromolar concentrations. Ltc2a adopts a helix–hinge–helix structure in membrane mimicking environment, whereas its derivative laticin 2aG11A (ltc2aG11A, GLFGKLIKFKARKAISYAVKKARGKH-COOH), likely adopts a more rigid structure, demonstrates stronger nonspecific interaction with the zwitterionic membrane, and is potentially more toxic against eukaryotic cells. In this work, interactions of these two ltc2a derivatives with supported “raft” lipid bilayer (1,2-dioleoyl-*sn*-glycero-3-phosphocholin/egg sphingomyelin/cholesterol 40/40/20 mol%) were studied by *in situ* atomic force microscopy in order to investigate the potential anticancer activity of the peptides since some breast and prostate cancer cell lines contain higher levels of cholesterol-rich lipid rafts than non-cancer cells. Both peptides induced reorganization of the raft model membrane by reducing line tension of the liquid ordered phase. Ltc2aG11A induced membrane thinning likely due to membrane interdigitation. Formation of large pores by the peptides in the bilayer was observed. Cholesterol was found to attenuate membrane disruption by the peptides. Finally, leakage assay showed that both peptides have similar membrane permeability toward various model membrane vesicles.

© 2012 Elsevier B.V. All rights reserved.

1. Introduction

Antimicrobial peptides (AMPs) are innate host defense components present in various organisms to defeat a wide spectrum of pathogens, including bacteria, viruses, and fungi. AMPs are typically short amphipathic peptides containing both cationic and hydrophobic amino acid residues [1–6]. Over 1200 AMPs have been discovered but the mechanisms of actions remain uncertain [4]. Various models—such as barrel-stave, toroidal, and carpet—have been proposed, with the Shai–Matuszaki–Huang model being the most comprehensive [3–6]. In summary, the Shai–Matuszaki–Huang model explains that the peptides carpet the membrane and the insertion causes area expansion of the outer leaflet and membrane thinning. The strain between outer and inner leaflets generates tension within the bilayers resulting in toroidal pores, which allow transportation of peptides and lipids into the inner leaflet. The peptides can then diffuse onto intercellular targets or cause physical disruption and collapse of membrane, both of which result in cell death [3].

Various studies have shown that AMPs share similar properties with cationic amphiphilic anticancer agents that can be categorized into two classes: agents toxic to both bacterial and cancer cells but not mammalian

non-cancer cells, and agents toxic to all cell types, including mammalian non-cancer cells [7,8]. Cancer cell membranes contain more anionic molecules, such as phosphatidylserine lipids and O-glycosylated mucins [7,8]. Thus cationic anticancer agents preferentially bind to such anionic membranes through nonspecific electrostatic interaction. In addition, cancer cells contain higher numbers of microvilli—minute projections of the cell membrane—providing a larger surface [7,8] and were also shown to be more fluid than membranes of normal cells, making them more susceptible for disruption by anticancer agents [9]. Thus differences in lipid composition, fluidity, and surface area between normal and cancer cell membranes contribute to the activity and efficiency of anticancer agents.

Recently, a new family of antimicrobial peptides called laticins was purified from the venom gland of the Central Asian spider *Lachesana tarabaevi* [10]. Seven structurally unrelated groups of short linear cysteine-free membrane-active peptides that are lytic to Gram-positive and Gram-negative bacteria, erythrocytes, and yeast at micromolar concentrations were identified [10]. A 26 amino acid residue peptide laticin 2a (ltc2a, GLFGKLIKFKGRKAISYAVKKARGKH-COOH) has broad-spectrum antibacterial activity against Gram-positive and Gram-negative bacteria with MIC values in the micromolar range [10], while having moderate hemolytic activity toward human erythrocytes with an EC₅₀ in the 3 to 6 μM range [11,12]. Both molecular dynamics simulation and NMR data indicate that ltc2a adopts a helix–hinge–helix structure in a small micelle with N-terminus helix embedded in the micelle and C-terminus laying on the membrane [13,14]. However, in a larger micelle, molecular dynamics simulations showed that two helices of ltc2a are angled 150° apart and lie peripherally on the membrane [14]. To investigate membrane binding

* Corresponding author. Tel.: +1 613 520 2600.

E-mail address: anatoli_ianoul@carleton.ca (A. Ianoul).

and rupturing by Itc2a, in a previous study we compared Itc2a to its mutant Itc2aG11A, GLFGKLIKFKFARKAISYAVKKARGKH-COOH and found that by replacing glycine 11 with alanine at the hinge region, a more rigid peptide with reduced conformational flexibility is obtained. The mutant Itc2aG11A has stronger nonspecific interaction with zwitterionic cell membranes, thus potentially leading to higher toxicity against eukaryotic cells [15].

It has been suggested that cholesterol in eukaryotic cell membranes prevents the cytolytic effect of antimicrobial agents [16]. Membranes with higher cholesterol levels had decreased rate of peptide insertion [17]. At the same time, Li et al. suggested that some breast and prostate cancer cell lines contain higher levels of cholesterol-rich lipid rafts than non-cancer cells [18], pointing at the relevance of raft supported lipid bilayers (SLBs) for modeling cancer cells. Enriched in cholesterol and sphingolipids, rafts have been characterized as detergent-resistant domains due to their insolubility in detergents such as Triton X-100 [19,20]. These microdomains are involved in regulating various cellular functions [18,19]. Therefore in this study we investigated the interactions of Itc2a derivatives with supported raft lipid bilayers and lipid vesicles in order to gain further understanding of the mechanism of action of Itc2a, and its cytotoxic and potential anticancer properties.

2. Materials and methods

1,2-Dioleoyl-*sn*-glycero-3-phosphoethanolamine (DOPE), 1,2-dioleoyl-*sn*-glycero-3-phospho-(1'-*rac*-glycerol) (sodium salt) (DOPG), 1,1',2,2'-tetramyristoyl cardiolipin (sodium salt) (CL), 1,2-dioleoyl-*sn*-glycero-3-phosphocholin (DOPC), egg sphingomyelin (SM), and cholesterol (Chol, ovine wool, >98%) were purchased from Avanti Polar Lipids Inc. (Alabaster, AL). Latarcin 2a (>95.1% purity) and ITC2a G11A (>95.4% purity) were synthesized by Gen Script Corporation (Piscataway, NJ). Stock solutions of the peptides were prepared in the required concentration in 18.2 MΩ cm⁻¹ Milli-Q water. 6-Carboxyfluorescein (CF) was from ACROS Organic (NJ). Calcein and ascorbic acid were from Sigma-Aldrich (Oakville, ON). Tris, EDTA, Triton X-100, and ammonium molybdate were purchased from Bioshop (Burlington, ON).

2.1. Liposome preparation

Five different model cell membranes were used: mammalian model (DOPE/DOPC/Chol 22.2/44.4/33.4 mol%), raft model (SM/DOPC/Chol 40/40/20 mol%), *Escherichia coli* model (*E. coli*, DOPE/DOPG 80/20 mol%), *Staphylococcus aureus* model (*S. aureus*, DOPG/CL 55/45 mol%) and *Bacillus subtilis* model (*B. subtilis*, DOPE/DOPG/CL 12/84/4 mol%) [21,22]. The liposomes were prepared by dissolving appropriate amounts of lipids in chloroform followed by solvent evaporation under a stream of nitrogen. The samples were kept in vacuum for at least 24 h to ensure complete removal of the solvent. The lipid films were hydrated for 30 min in Milli-Q water or leakage buffer (10 mM Tris-HCl, 150 mM NaCl, 1 mM EDTA pH 7.45) containing 70 mM CF/calcein, for AFM imaging and leakage assay, respectively, to obtain the final lipid concentration 1 mg/mL. The hydration temperature was 50 °C for raft model and 40 °C for other model membranes. For AFM imaging, lipid suspension was vigorously stirred followed by sonication with Elma S10H Elmasonic at 50 °C. For leakage assay, the lipid suspension was sonicated at 40 °C for 5 min followed by extrusion through 200 nm polycarbonate membrane (Nuclepore Track-Etch membrane, Whatman) 31 times at 40 °C. Five freeze/thaw cycles were then performed to maximize CF/calcein encapsulation. Free CF/calcein was separated with a Sephadex G-50 size exclusion column using leakage buffer for equilibrium and elution.

2.2. Atomic force microscopy (AFM) imaging

Topography images of supported lipid bilayers were obtained in contact mode with an Ntegra (NTMDT, Russia) atomic force microscope at

room temperature with 512 × 512 points per image and 0.7 Hz scanning rate. A 100 × 100 μm² scanner and rotated monolithic silicon cantilevers (450 μm-long, force constant 0.2 N/m ContAl, resonance frequency 13 kHz; Budget Sensor) or silicon nitride V-shaped cantilevers (100 μm-long, force constant 0.27 N/m, 30 kHz; Budget Sensor). The supported lipid bilayers were formed on freshly cleaved mica substrates sealed with a silicon O-ring in a fluid cell by adding 1 mL PBS, 40 μL of 1 M CaCl₂ and 1 mL of 1 mg/mL lipid vesicles. After incubating at room temperature for 50 min, the fluid cell was rinsed with Milli-Q deionized water or with 150 mM NaCl solution to remove excess vesicles. To investigate the role of cholesterol model cell membranes composed of DOPC/SM 50/50 mol% was used. Peptide was injected directly into the fluid cell by incrementally adding 15 μL of 0.29 mg/mL solution (this corresponds to increasing the total peptide concentration in the 2 mL cell by 0.3 μM) up to 0.9 μM.

AFM images (10 × 10 μm²) were threaded into sequential video (1 s per frame with 0.9 s cross dissolve transition between each image) using an iMovie application. The Z scale in the images was ~6 nm; for some final images in the videos ~20 nm. Scale bar in each video is 2 μm.

2.3. Leakage assay

Leakage experiments were performed as described previously [23] by using 2 mL of CF or calcein-containing vesicles diluted 20 times with the leakage buffer on a Varian Cary Eclipse spectrofluorometer. Excitation and emission wavelengths were between 475 to 490 nm, and 510 to 525 nm, respectively, slits were 2.5 nm, and integration time was 1.5 s. The baseline fluorescence (F₀) was monitored until steady signal intensity was reached before the addition of peptide. After the peptide was added, the fluorescence signal intensity was monitored for 10 min or until no further changes were observed. The final fluorescence signal intensity (F) was then measured. The maximum fluorescence signal that corresponds to complete the disruption of the vesicles (F_M) was measured by adding 20 μL of 10% triton X-100 to the mixture at the end of each experiment. Fluorescence intensity was monitored for 5 min. The following formula was used to measure the leakage fraction: % leakage = [(F - F₀) × 100%] / (F_M - F₀). Lipid phosphorus concentration was determined using a phosphate assay [24].

3. Results and discussion

3.1. Raft domains in supported lipid bilayers visualized by atomic force microscopy

The formation of microscale domains in the raft mixture has been extensively studied over the past decade. It is now well established that sphingomyelin can form both inter- and intra-molecular hydrogen bonds with other lipids and cholesterol whereas phosphocholine (PC) lipid could only be the acceptor for hydrogen bonding [25,26]. In addition, intramolecular hydrogen bonding between SM molecules also limits the lateral diffusion and rotational motion of SM and indirectly strengthens the interaction with Chol [25]. Moreover, Chol preferentially interacts with SM and other sphingolipids due to their structure and the saturation of the hydrocarbon chain [27]. As a result when supported by a freshly cleaved mica SM/DOPC/Chol forms a phase separated SLBs with SM and Chol in liquid ordered (L_o) phase that is 0.5–1 nm higher than DOPC in the liquid disordered (L_d) phase (Fig. 1) [20,25,27–29]. The location and size of domains remain relatively constant over the 60 min period after the addition of 30 μL of deionized water or 150 mM NaCl solution. However, the detergent resistant 5 nm domains were visualized after treatment with 0.28 mM Triton X-100 (Fig. 1), consistent with previous studies [20,30]. These supported lipid bilayers therefore represent a convenient model to investigate the activity of various bioactive peptides, such as ITC2a.

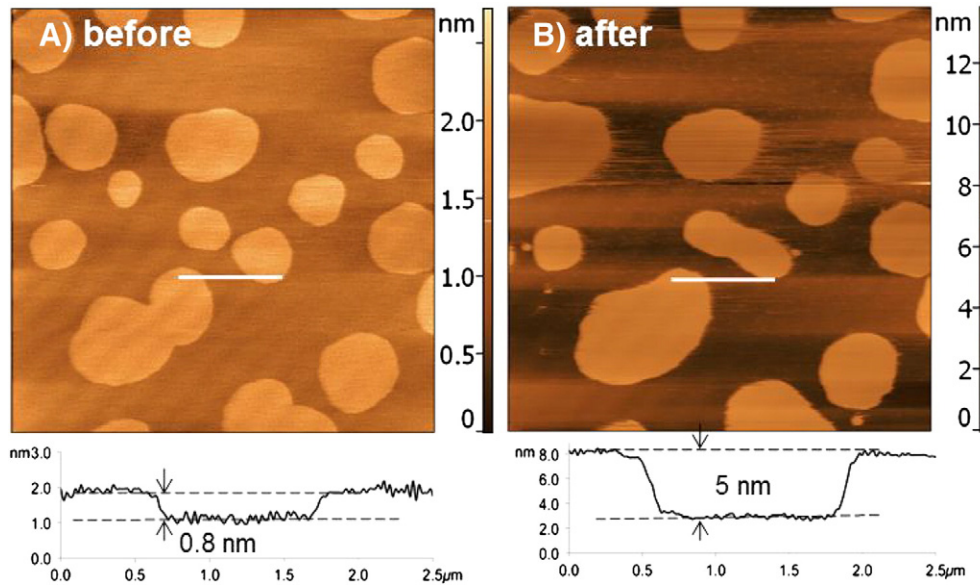


Fig. 1. AFM topography images ($10 \times 10 \mu\text{m}^2$) of DOPC/SM/Chol 40/40/20 mol% SLBs before (A) and after (B) the addition of $0.28 \mu\text{M}$ Triton X-100 in 150 mM NaCl medium at room temperature.

3.2. Peptides reduce line tension and reorganize morphology of supported lipid bilayer

A number of studies have shown that peptides preferentially insert into loosely packed L_d phase than into L_o domains and change raft morphology [28,31,32]. For example, addition of an antimicrobial peptide indolicidin and cell-penetrating peptide TAT remodeled raft SLBs by

reducing the line tension and causing lipid association [28]. Binding and insertion of apoptosis regulator Bax-derived peptide to raft SLBs released curvature stress at the domain interface causing domain expansion [31]. Addition of a myristoylated cationic peptide for neuronal growth and plasticity NAP-22 caused L_o domains to coalesce [32].

As Itc2a was shown to be toxic to human erythrocytes as well as to erythroleukemia K562 cells with EC_{50} values $3.4 \mu\text{M}$ and $3.3 \mu\text{M}$,

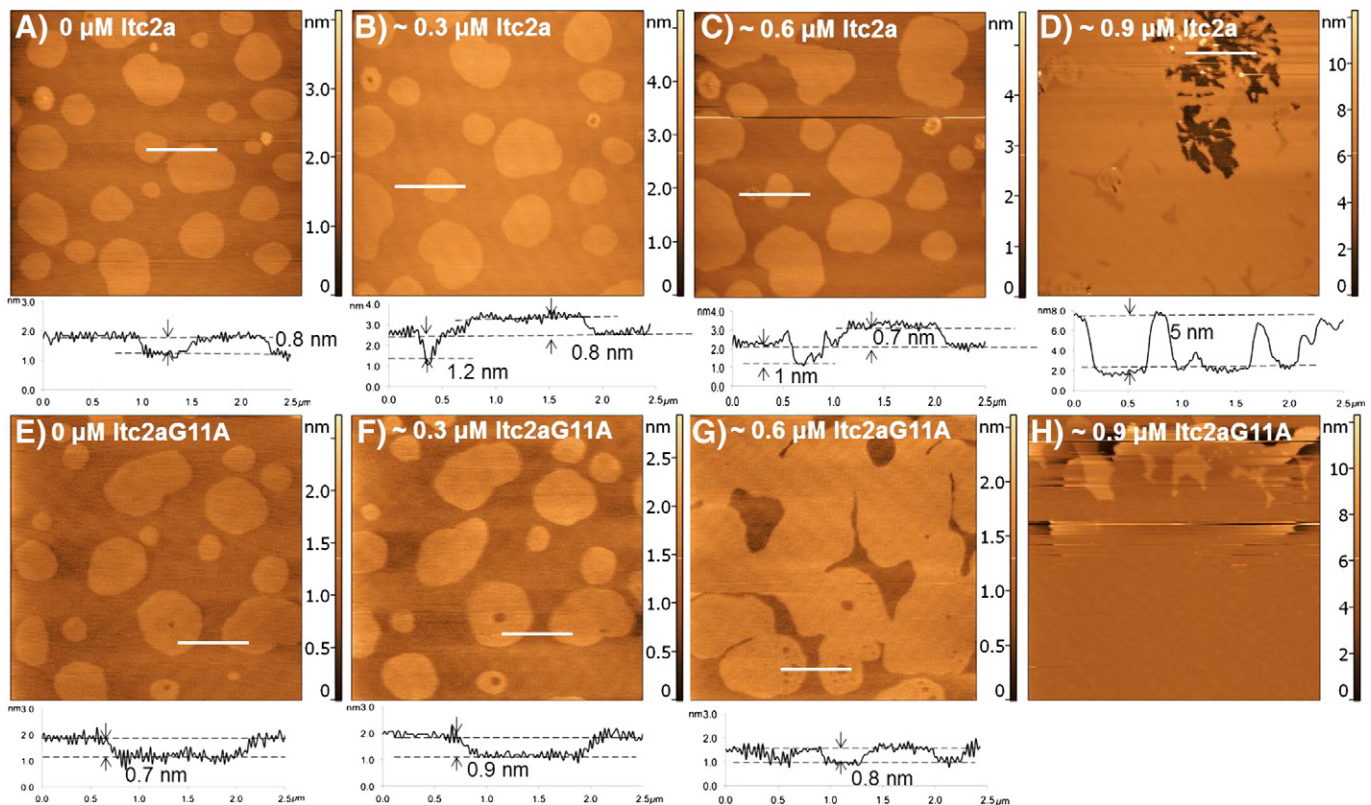


Fig. 2. AFM topography images ($10 \times 10 \mu\text{m}^2$) of DOPC/SM/Chol 40/40/20 mol% SLBs with Itc2a (upper row) and Itc2aG11A (bottom row) in 150 mM NaCl medium at room temperature. (A, E) Before addition; (B, F) $0.3 \mu\text{M}$; (C, G) $0.6 \mu\text{M}$; (D, H) $0.9 \mu\text{M}$.

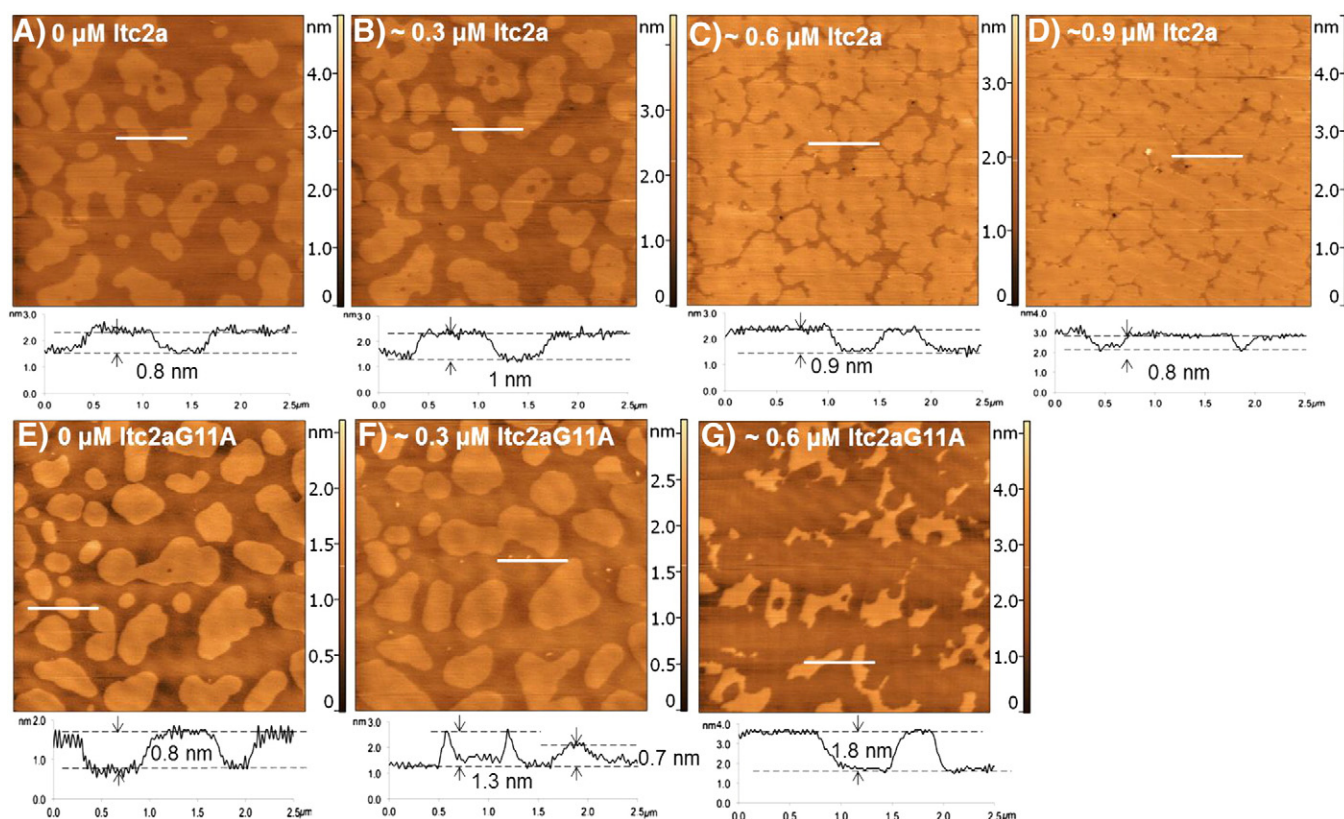


Fig. 3. AFM topography images ($10 \times 10 \mu\text{m}^2$) of DOPC/SM/Chol 40/40/20 mol% SLBs with ltc2a (upper row) and ltc2aG11A (bottom row) in deionized water at room temperature. (A, E) Before addition; (B, F) 0.3 μM ; (C, G) 0.6 μM ; (D) 0.9 μM of ltc2a.

respectively [11], it can be considered a potential anticancer agent. The peptide demonstrated time and stage dependent erythrocyte membrane reorganization leading to the formation of pores 2 to 13 nm in diameter. In the case of cancer K562 cells, ltc2a insertion induced bleb formation and swelling accompanied by formation of ~ 4 nm pores leading to membrane disintegration [11]. Therefore, it was of interest to investigate the effect of both ltc2a derivatives on the raft SLBs.

The measurements were performed in deionized water and in 150 mM NaCl, since the antimicrobial activity of some peptides was found to depend on salt concentration [33–37]. Before the peptide addition raft bilayers contained circular L_0 domains (Figs. 2–5, A, E, and Videos

1–8, initial frames) indicating that among the factors affecting domain size distribution (line tension, entropy, and electrostatic interaction [38,39]), line tension is the dominant.

The peptide was then added to the model bilayer and sequential images were recorded. The first set of measurements was performed by incrementally increasing the peptide concentration in the solution from 0.3 to 0.9 μM (Figs. 2–3, Videos 1–4). Initially after the peptide addition small aggregates or pores appear in the L_d phase (Fig. 3B and F), and subsequently L_0 domains become irregular, expand and coalesce (Figs. 2D, G, 3C, F, Videos 1–4) suggesting reduction in line tension. The effect becomes more apparent with time and increasing peptide concentration. It also appears that the morphology changes faster in deionized water

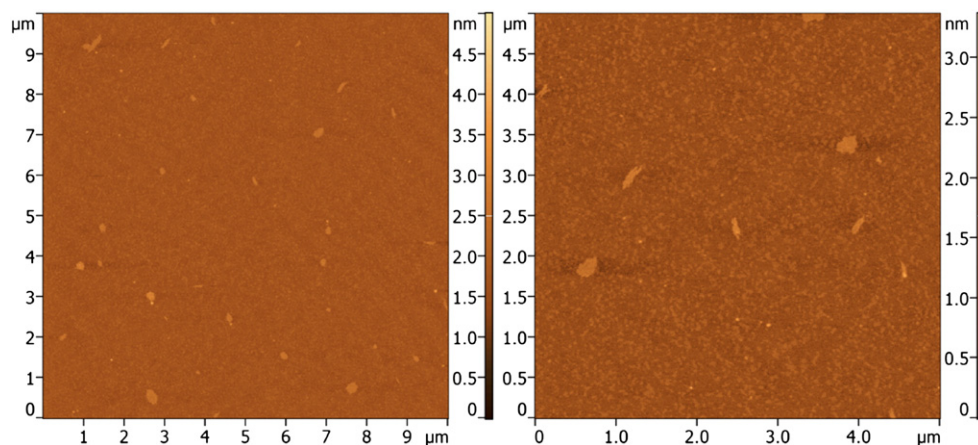


Fig. 4. AFM topography images of laticin 2a deposited from 0.9 μM aqueous solution on mica and imaged in air.

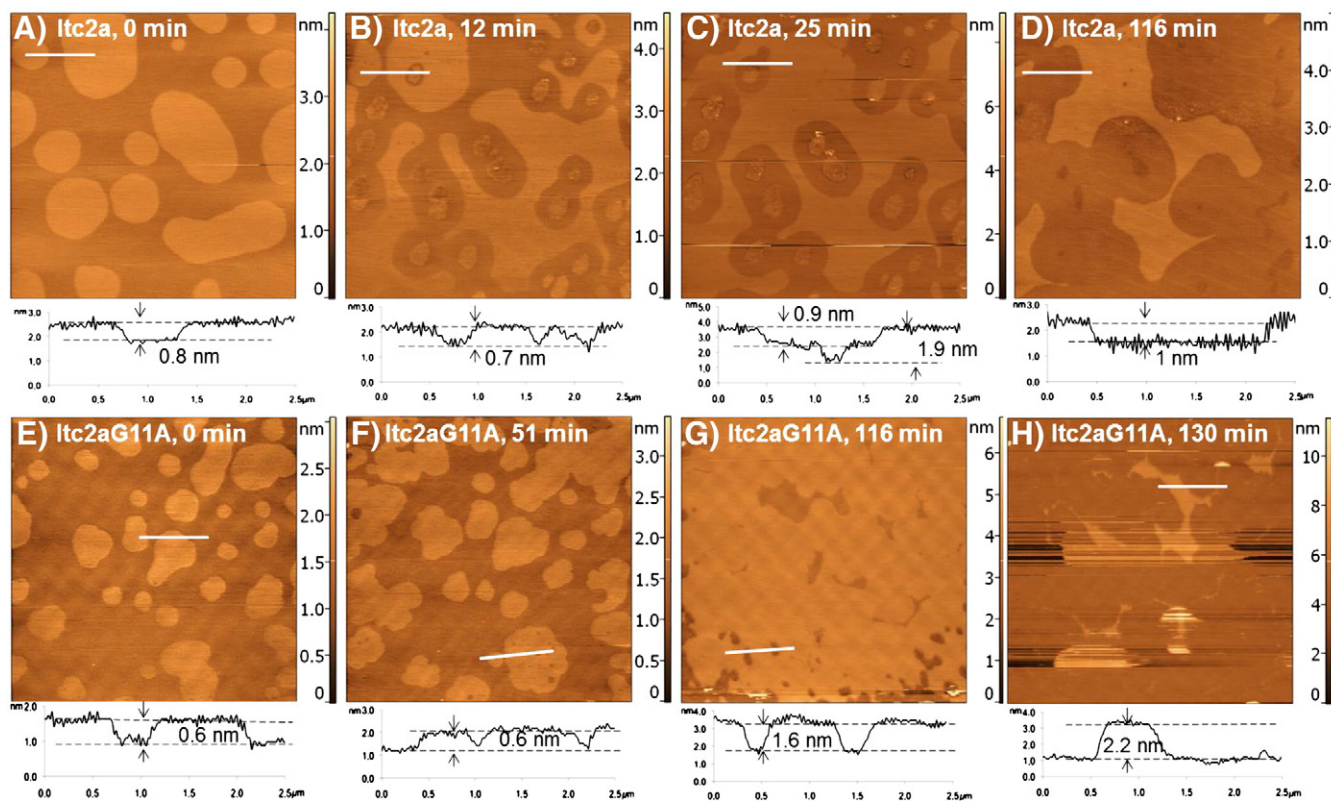


Fig. 5. AFM topography images ($10 \times 10 \mu\text{m}^2$) of DOPC/SM/Chol 40/40/20 mol% SLBs with 0.6 μM Itc2a (A–D) and Itc2aG11A (E–H) in 150 mM NaCl medium at room temperature. (A, E) 0 min; (B, F) 12 min; (C, G) 25 min; (D, H) 116 min; (F) 51 min; (H) 130 min.

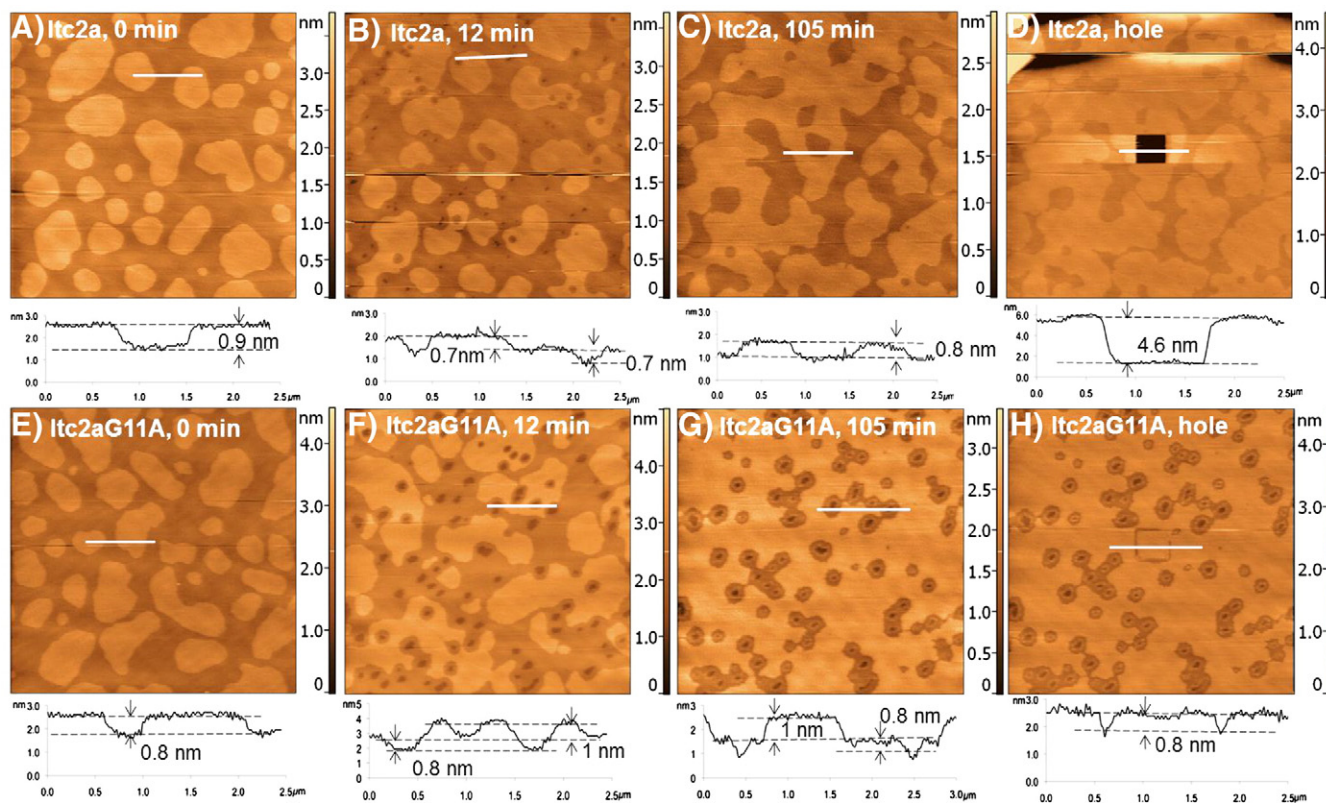


Fig. 6. AFM topography images ($10 \times 10 \mu\text{m}^2$) of DOPC/SM/Chol 40/40/20 mol% SLBs with 0.6 μM Itc2a (A–D) and Itc2aG11A (E–H) in deionized water at room temperature. (A, E) 0 min; (B, F) 12 min; (C, G) 105 min; (D, H) $1 \times 1 \mu\text{m}^2$ after scanning with high force and speed.

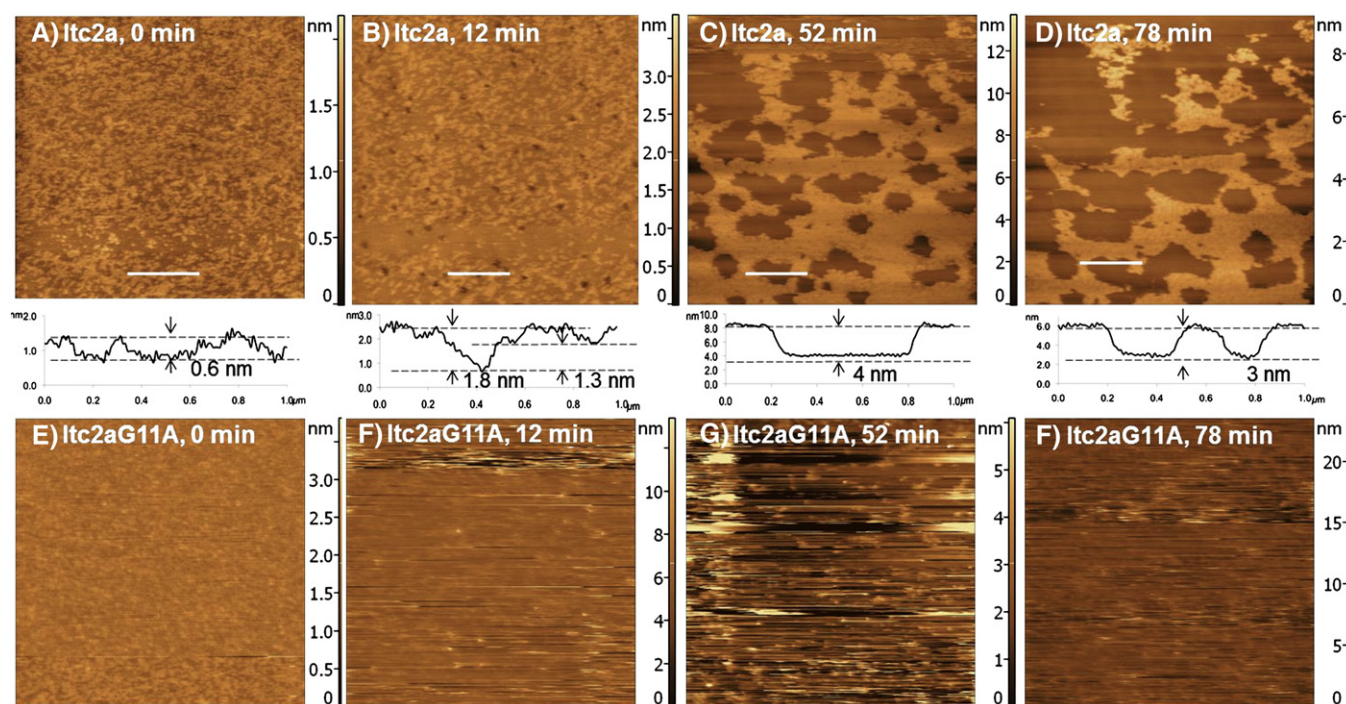


Fig. 7. AFM topography images ($5 \times 5 \mu\text{m}^2$) of DOPC/SM 1:1 SLBs after addition of $0.6 \mu\text{M}$ ltc2a (A–D) and $0.3 \mu\text{M}$ ltc2aG11A (E–H) in deionized water at room temperature. (A, E) 0 min, (B, F) 12 min, (C, G) 52 min, (D, H) 78 min.

(Fig. 3C, G, Videos 2, 4) than in high salt medium (Fig. 2C, G, Videos 1, 3), and for ltc2aG11A (Figs. 2G, 3G, Videos 1, 3) than for ltc2a. Association with the peptide causes an imbalance of uniformly distributed lipid molecules; therefore lipid bilayer reorganizes to restore new equilibrium between the peptide and the lipid.

Detected morphological changes of the bilayer were somewhat different in high salt medium (150 mM NaCl). For example, in the case of ltc2aG11A, both cluster formation and disruption started in L_d phase (Fig. 3F, G, and Video 1) in deionized water but not in NaCl medium (Fig. 2F, and Video 3). It is known that NaCl compacts lipid bilayers with sodium ions tightly bound to the carbonyl oxygen of, on average, three lipid molecules [40,41]. This reversible process has been observed in SLB composed of various lipids such as PC, POPE, and *E. coli* lipid extract [42]. Previous studies have also shown that sodium ions strongly interact with carbonyl oxygen in the peptide backbone and carboxylate group of amino acid side chain [43,44]. This decreases the hydrogen bonding of peptide with water and therefore the peptide preferentially inserts into the hydrophobic environment. Thus in the presence of NaCl, the peptide may deform which can facilitate the formation of complex with lipid molecules, followed by distortion and solubilization of SLB.

Results of the present AFM experiments confirm membrane disintegration by ltc2a (Figs. 2D, H, 3G, and Videos 1–4) observed before [11]. However, no previously mentioned small pores were detected, likely due to limitations of AFM imaging.

3.3. Oligomerization may contribute to the peptide activity

In our previous preliminary study small aggregates of laticin 2a in phospholipid bilayer surface were detected [15]. Similar aggregates were also observed in the present study (for example, Fig. 3F and Video 1 at 142 min) suggesting the potential role of peptide clustering on the activity of laticins. Such oligomerization was found to affect the selective binding of NAP-22 peptide to cholesterol rich domains [45].

When deposited from a $0.9 \mu\text{M}$ solution onto freshly cleaved mica and imaged in air ltc 2a was found to form small nanoscale aggregates 1–1.5 nm high (Fig. 4). Therefore, in the second set of experiments

the peptides were added to the bilayer in higher initial concentration ($0.6 \mu\text{M}$) (Figs. 5, 6, Videos 5–8) to test the effect of potential laticin oligomerization on the bilayer. At this peptide concentration disruption dynamics is fairly slow, enabling time resolved AFM studies of laticin activity (Videos 1–4).

Upon peptide addition L_o domains expanded and coalesced both in NaCl (Fig. 5, Videos 7, 8) and in deionized water (Fig. 6, Videos 5, 6), similar to experiments with peptide at lower concentration. However, some differences between the two were observed.

In the NaCl medium, ltc2a formed clusters in both L_o and L_d phases while the L_o phase expanded and coalesced around the clusters. This was followed by slow L_o cluster dissociation and membrane solubilization (Fig. 5A–D, Video 8). Without NaCl compacting SLBs, ltc2a created defects and solubilized both L_d and L_o phases, followed by slow L_o domain expansion and coalescence (Fig. 6A–C, Video 6). By scanning a $1 \times 1 \mu\text{m}^2$ area with high speed and high force we were able to obtain a 5 nm deep hole for ltc2a/bilayer in deionized water indicating that ltc2a “freezes” the zwitterionic SLBs after peptide/lipid complex formation (Fig. 6D) as described by Polyansky et al. [14].

In comparison, ltc2aG11A in NaCl medium does not form pores or defects (Fig. 5E–H, Video 7), whereas in aqueous solution it immediately forms stable pores in L_d phase followed by rapid L_o domain expansion and coalescence (Fig. 6E–G, Video 5). It is qualitatively similar to the behavior of ltc2a in NaCl medium, although on a smaller scale. In the case of ltc2aG11A, the SLBs appeared to be more fluid as a 5 nm deep “hole” could not be obtained and was covered by the expanded L_o phase (Fig. 6H).

Thus, when the initial peptide concentration in solution is increased, some variations in the mechanism of action are detected suggesting potential initial peptide aggregation in solution followed by dissociation in a membrane.

3.4. ltc2aG11A induced membrane thinning

An interesting observation was made for ltc2aG11A in deionized water. Large (50–100 nm) stable pores were detected after the addition of $\sim 0.6 \mu\text{M}$ ltc2aG11A to the raft SLBs (Fig. 6F–H, Video 5). A reduction

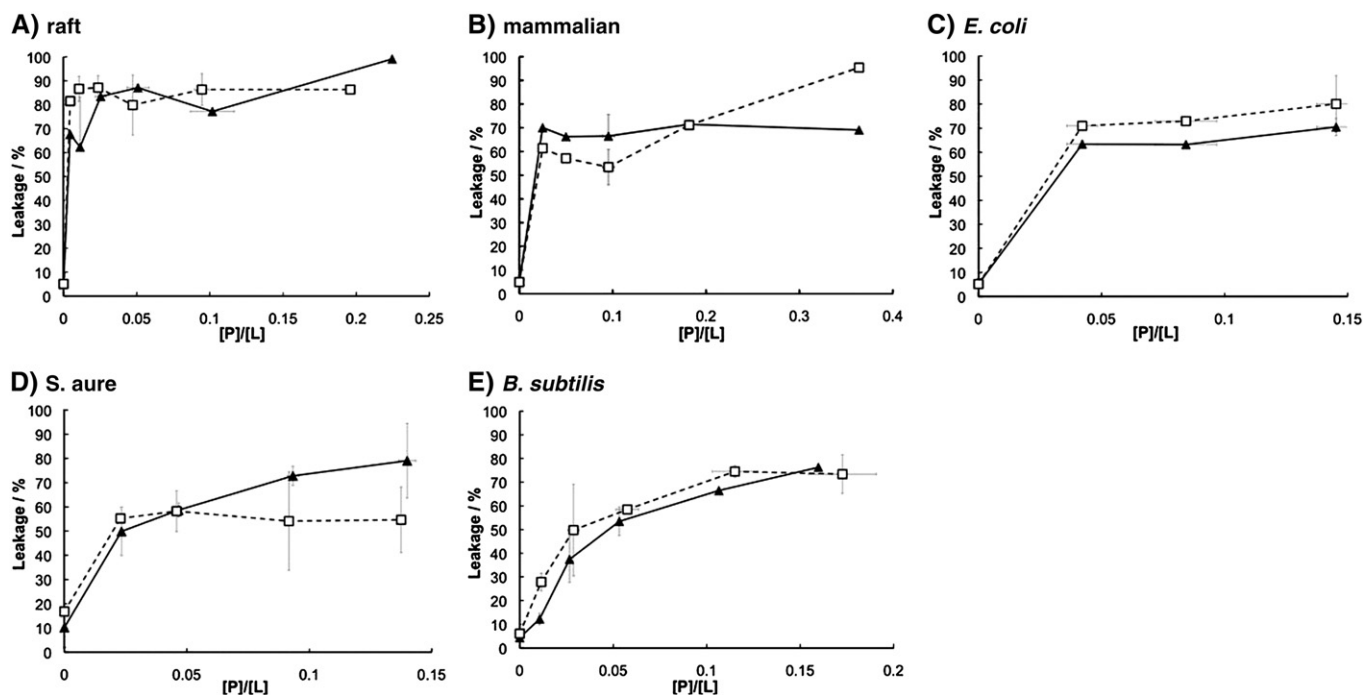


Fig. 8. Carboxyfluorescein/calcein signal increase after addition of ltc2a (closed triangle) and ltc2aG11A (open square) to (A) raft (DOPC/SM/Chol 40/40/20 mol%), (B) mammalian (DOPE/DOPC/Chol 22.2/44.4/33.4 mol%), (C) *E. coli* (DOPE/DOPG 80/20 mol%), (D) *S. aureus* (DOPG/CL 55/45 mol%) and (E) *B. subtilis* (DOPE/DOPG/CL 12/84/4 mol%) model LUVs.

in the membrane thickness was also observed before complete membrane solubilization in all cases (Figs. 3G, 5H, Videos 1, 3, 7). After scanning a small area with high force through an extended period of time, for example following the Fig. 3H image, we were unable to see any traces (unlike Fig. 6D and H) suggesting that the lower phase is mica rather than L_d phase of the lipid bilayer. Therefore, we concluded that after the addition of ltc2aG11A membrane thinning occurs followed by complete membrane solubilization. The thickness of the remaining L_o domains is in the range of 1.8 to 2.2 nm (Figs. 3G and 4H). This is more than a lipid head group (~0.9 nm) or a single helix (1.1 to 1.5 nm) [15,46]. At the same time it is less than a single monolayer of ~2.5 nm. Membrane thinning has been previously observed for various peptides: magainin 2, gramicidin, MSI-78, indolicidin, curcumin, and saposin C [28,46–50]. The underlying mechanism of peptide-induced membrane thinning includes membrane interdigitation, complex formation between a single leaflet and peptides, and peptide induced asymmetric bilayer with lipid flip-flop [29]. It is unclear what mechanism is responsible for membrane thinning in the present study. However previous studies indicated membrane thickness of 1.5 to 1.9 nm for interdigitated domains [47] suggesting this as the preferred mechanisms for ltc2aG11A.

3.5. Cholesterol attenuated the effect of the peptides

Interactions between laticins and bilayers composed of DOPC/SM 1:1 was investigated to observe the effect of Chol on ltc2a activity. The morphology of the bilayer in the absence of peptides (Fig. 7A, E) is similar to that observed previously [51]. When ltc2a was added in a final concentration of 0.6 μ M defects in the DOPC phase of the bilayer were observed (Fig. 7B). The size of the defects increased with time. SM domains (higher phase) coalesced and eventually were solubilized (Fig. 7C, D). In the case of ltc2aG11A, the peptide disrupted DOPC/SM bilayer already at 0.3 μ M. Cholesterol is known to induce the formation of micrometer size L_o phase domains with SM in biological membranes. Previous studies have shown that cholesterol decreased binding and insertion of some antimicrobial peptides—and thus decreased their antimicrobial activities—even in the presence of anionic lipids [52–54]. This could explain the

disappearance of defects in raft SLBs (Fig. 6B) while the defects in DOPC/SM SLBs formed and increased in size (Fig. 7B).

3.6. Leakage assay demonstrated the antimicrobial and hemolytic activity of both peptides

Laticins are known to exhibit antimicrobial and hemolytic activity, and have different specificities [11]. To measure the lytic activities of ltc2a and ltc2aG11A on five model membranes in vesicles, leakage assay was used. To assess the magnitude of their antimicrobial spectrum both laticins were tested against the following model membranes: gram-negative bacterium *E. coli*, and gram-positive bacteria, *S. aureus* (methicillin-resistant *S. aureus*—MRSA) and *B. subtilis*. The mammalian model was chosen as a positive control, representative of human red blood cells [55], and the raft model was chosen to represent cancer cells, as cancer cells are more abundant in lipid rafts than healthy cells [18]. It was found that both peptides have lytic activities on all five membranes (Fig. 8). This is observed by the increase in fluorescence measured from the sample upon peptide addition, which infers fluorescent dye leakage from the ruptured lipid vesicles. When it comes to bacterial model membranes, ltc2a was found to have high lytic activity, and performed similarly with all three. ltc2aG11A was also found to have high lytic activity, although slightly greater than ltc2a, towards *E. coli* and *B. subtilis* but lower towards *S. aureus* (Fig. 8C, D, and E). This could suggest that the lytic activity of ltc2aG11A is correlated with the content of DOPE; replacing glycine at position 11 with alanine does not lead to a decrease in amphipathicity but does result in a more rigid structure that interacts with zwitterionic model cell membranes more efficiently, thus explaining higher activity [15]. This was also shown with the peptide piscidin 1 when two glycines were replaced with alanines [56].

There was no notable difference between the activities of both peptides toward the raft model membrane at high peptide concentrations, however, at low concentrations ltc2aG11A showed slightly stronger lytic activity (Fig. 8A). Yet, in comparison to the mammalian model (Fig. 8B), both peptides had greater lytic activity toward the raft model. This suggests that the presence of SM may have a stronger effect on the peptides activity than DOPE. As discussed earlier and observed in *in situ*

AFM, SM promotes peptides aggregation and the formation of irreversible transmembrane pores, which could contribute to higher leakage in the raft model. Overall, the data of leakage assay correlate sufficiently well with the AFM measurements.

4. Conclusion

In this work, we examined the role of the hinge in ltc2a peptide by *in situ* AFM and vesicle leakage assay. Both laticin 2a derivatives induced membrane reorganization by reducing line tension of the liquid ordered phase upon association of the peptides. The presence of 150 mM NaCl did not notably decrease the peptide activity but slightly altered the mode of action. Ltc2aG11A induced raft membrane thinning possibly due to membrane interdigitation. Both laticin 2a derivatives are likely to form oligomers in solution that may alter the mechanism of peptide action. Cholesterol was found to attenuate peptide-induced membrane disruption. This observation somewhat contradicting previously observed anticancer activity of ltc2a, suggests that other factors in the membrane structure of cancer cells, for example charge, increased surface area, or morphology rather than higher abundance of cholesterol are responsible for such peptide activity. More rigid ltc2aG11A exhibited slightly higher membrane lytic activity than the wild type ltc2a.

Supplementary data to this article can be found online at <http://dx.doi.org/10.1016/j.bbame.2012.07.030>.

Acknowledgements

Financial support was provided by Early Researcher Award, Ontario Graduate Scholarship, and the Canadian Foundation for Innovation.

References

- [1] M.R. Yeaman, N.Y. Yount, Mechanisms of antimicrobial peptide action and resistance, *Pharmacol. Rev.* 55 (2003) 27–55.
- [2] R.E.W. Hancock, H.-G. Sahl, Antimicrobial and host-defense peptides as new anti-infective therapeutic strategies, *Nat. Biotechnol.* 24 (2006) 1551–1557.
- [3] M. Zasloff, Antimicrobial peptides of multicellular organisms, *Nature* 415 (2002) 389–395.
- [4] Y. Lai, R.L. Gallo, AMPed up immunity: how antimicrobial peptides have multiple roles in immune defense, *Trends Immunol.* 30 (2009) 131–141.
- [5] W.C. Wimley, Describing the mechanism of antimicrobial peptide action with the interfacial activity model, *ACS Chem. Biol.* 5 (2010) 905–917.
- [6] K.A. Brogden, Antimicrobial peptides: pore formers or metabolic inhibitors in bacteria? *Nat. Rev. Microbiol.* 3 (2005) 238–250.
- [7] F. Schweizer, Cationic amphiphilic peptides with cancer-selective toxicity, *Eur. J. Pharmacol.* 625 (2009) 190–194.
- [8] D.W. Hoskin, A. Ramamoorthy, Studies on anticancer activities of antimicrobial peptides, *Biochim. Biophys. Acta* 1778 (2008) 357–375.
- [9] M. Sok, M. Sentjurs, M. Schara, Membrane fluidity characteristics of human lung cancer, *Cancer Lett.* 139 (1999) 215–220.
- [10] S.A. Kozlov, A.A. Vassilevski, A.B. Feofanov, A.Y. Surovov, D.V. Karpunin, E.V. Grishin, Laticins, antimicrobial and cytolytic peptides from the venom of the spider *Lachesana tarabaevi* (Zodariidae) that exemplify biomolecular diversity, *J. Biol. Chem.* 281 (2006) 20983–20992.
- [11] O.B. Vorontsova, N.S. Egorova, A.S. Arseniev, A.V. Feofanov, Haemolytic and cytotoxic action of laticin ltc2a, *Biochimie* 93 (2011) 227–241.
- [12] A.A. Polyansky, A.A. Vassilevski, P.E. Volynsky, O.V. Vorontsova, O.V. Samsonova, N.S. Egorova, N.A. Krylov, A.V. Feofanov, A.S. Arseniev, E.V. Grishin, R.G. Efremov, N-terminal amphipathic helix as a trigger of hemolytic activity in antimicrobial peptides: a case study in laticins, *FEBS Lett.* 583 (2009) 2425–2428.
- [13] P.V. Dubovskii, P.E. Volynsky, A.A. Polyansky, V.V. Chupin, R.G. Efremov, A.S. Arseniev, Spatial structure and activity mechanism of a novel spider antimicrobial peptide, *Biochemistry* 45 (2006) 10759–10767.
- [14] A.A. Polyansky, P.E. Volynsky, R.G. Efremov, Computer simulations of membrane-lytic peptides: perspectives in drug design, *J. Bioinform. Comput. Biol.* 5 (2007) 611–626.
- [15] G. Idiong, A. Won, A. Ruscito, B.O. Leung, A.P. Hitchcock, A. Ianoul, Investigating the effect of a single glycine to alanine substitution on interactions of antimicrobial peptide laticin 2a with a lipid membrane, *Eur. Biophys. J.* 40 (2011) 1087–1100.
- [16] C. Leuschner, W. Hansel, Membrane disrupting lytic peptides for cancer treatments, *Curr. Pharm. Des.* 10 (2004) 2299–2310.
- [17] H. Steiner, D. Andreu, R.B. Merrifield, Binding and action of ceropin and ceropin analogues: antibacterial peptides from insects, *Biochim. Biophys. Acta* 939 (1988) 260–266.
- [18] Y.C. Li, M.J. Park, S.-K. Ye, C.-W. Kim, Y.-N. Kim, Elevated levels of cholesterol-rich lipid rafts in cancer cells are correlated with apoptosis sensitivity induced by cholesterol-depleting agents, *Am. J. Pathol.* 168 (2006) 1107–1118.
- [19] T. Baumgart, S.T. Hess, W.E. Webb, Imaging coexisting fluid domains in biomembrane model coupling curvature and line tension, *Nature* 425 (2003) 821–824.
- [20] H.A. Rinia, M.M.E. Snel, J.P.J.M. van der Eerden, B. de Kruijff, Visualizing detergent resistant domains in model membranes with atomic force microscopy, *FEBS Lett.* 501 (2001) 92–96.
- [21] I. Ira, L.J. Johnston, Ceramide promotes restructuring of model raft membranes, *Langmuir* 22 (2006) 11284–11289.
- [22] R.F. Epand, P.B. Savage, R.M. Epand, Bacterial lipid composition and the antimicrobial efficacy of cationic steroid compounds (Ceragenins), *Biochim. Biophys. Acta* 1768 (2007) 2500–2509.
- [23] A. Won, A. Ianoul, Interactions of antimicrobial peptide from C-terminus of myotoxin II with phospholipid mono- and bilayers, *Biochim. Biophys. Acta* 1788 (2009) 2277–2283.
- [24] P.S. Chen, T.Y. Toribara Jr., H. Warner, Microdetermination of phosphorus, *Anal. Chem.* 28 (1956) 1756–1758.
- [25] R.M.A. Sullan, J.K. Li, C. Hao, G.C. Walker, S. Zou, Cholesterol-dependent nanomechanical stability of phase-segregated multicomponent lipid bilayer, *Biophys. J.* 99 (2010) 507–516.
- [26] M. Lonnfors, J.P.F. Doux, J.A. Killian, T.K.M. Nuholm, J.P. Slotte, Sterols have higher affinity for sphingomyelin than for phosphatidylcholine bilayers even at equal acyl-chain order, *Biophys. J.* 100 (2011) 2633–2641.
- [27] L.J. Pike, The challenge of lipid rafts, *J. Lipid Res.* 50 (2009) S323.
- [28] J.E. Shaw, R.F. Epand, J.C.Y. Hsu, G.C.H. Mo, R.M. Epand, C.M. Yip, Cationic peptide-induced remodeling of model membranes: direct visualization by *in situ* atomic force microscopy, *J. Struct. Biol.* 162 (2008) 121–138.
- [29] J.E. Shaw, J.-R. Alattia, J.E. Berity, G.G. Prive, C.M. Yip, Mechanism of antimicrobial peptide action: studies of indolicidin assembly at model membrane interfaces by *in situ* atomic force microscopy, *J. Struct. Biol.* 154 (2006) 42–58.
- [30] K. El Kirat, S. Morandat, Cholesterol modulation of membrane resistance to triton X-100 explored by atomic force microscopy, *Biochim. Biophys. Acta* 1768 (2007) 2300–2309.
- [31] A.J. Garcia-Saez, S. Chiantia, J. Salgado, P. Schwille, Pore formation by Bax-derived peptide: effect on the line tension of the membrane probed by AFM, *Biophys. J.* 93 (2007) 103–112.
- [32] P.-H. Puench, N. Borghi, E. Karatekin, F. Brochard-Wyart, Line thermodynamics: adsorption at a membrane edge, *Phys. Rev. Lett.* 90 (2003) 128304.
- [33] K. Konno, M. Hisada, R. Fontana, C.C.B. Lorenzi, H. Naoki, Y. Itagaki, A. Miwa, N. Kawai, Y. Nakrata, T. Yasuhara, J. Ruggiero Neto, W.F. de Azevedo Jr, M.S. Palma, T. Nakajima, Anoplin, a novel antimicrobial peptide from the venom of the solitary wasp *Anoplius samariensis*, *Biochim. Biophys. Acta* 1550 (2001) 70–80.
- [34] J. Tuner, C. Yoon, D. Nhu-Nguyen, A.J. Waring, L.I. Robert, Activities of LL-37, a cathelin-associated antimicrobial peptide of human neutrophils, *Antimicrob. Agents Chemother.* 42 (1998) 2206–2214.
- [35] J.P. Tam, Y.-A. Lu, J.-L. Yang, K.-W. Chiu, An unusual structural motif of antimicrobial peptides containing end-to-end macrocycle and cysteine-knot disulfides, *Proc. Natl. Acad. Sci. U. S. A.* 96 (1999) 8913–8918.
- [36] S.M. Travis, N.N. Anderson, W.R. Forsyth, C. Espirito, B.D. Conway, E.P. Greenberg, P.B. McCray Jr., R.I. Lehrer, M.J. Welsh, B.F. Tack, Bacterial activity of mammalian cathelicidin-derived peptides, *Infect. Immun.* 68 (2000) 2748–2755.
- [37] C. Friedrich, M.G. Scott, N. Karunaratne, H. Yan, R.E.W. Hancock, Salt-resistant alpha-helical cationic antimicrobial peptides, *Antimicrob. Agents Chemother.* 43 (1999) 1542–1548.
- [38] P.I. Kuzmin, S.A. Akimov, Y.A. Chizmadzhev, J. Zimmerberg, F.S. Cohen, Line tension and interaction energies of membrane rafts calculated from lipid splay and tilt, *Biophys. J.* 88 (2005) 1120–1133.
- [39] A.J. Garcia-Saez, S. Chiantia, P. Schwille, Effect of line tension on the lateral organization of lipid membrane, *J. Biol. Chem.* 282 (2007) 33537–33544.
- [40] R.A. Bockmann, A. Hac, T. Heimbürg, H. Grubmüller, Effect of sodium chloride on a lipid bilayer, *Biophys. J.* 85 (2003) 1647–1655.
- [41] G. Oncins, S. Garcia-Manyes, F. Sanz, Study of frictional properties of a phospholipid bilayer in a liquid environment with lateral force microscopy as a function of NaCl concentration, *Langmuir* 21 (2005) 7373–7379.
- [42] S. Garcia-Manyes, G. Oncins, F. Sanz, Effect of ion-binding and chemical phospholipid structure on the nanomechanics of lipid bilayer studied by force spectroscopy, *Biophys. J.* 89 (2005) 1812–1826.
- [43] E.G. Aziz, N. Ottosson, S. Eisebitt, W. Eberhardt, B. Jagoda-Cwiklik, R. Vacha, P. Jungwirth, B. Winter, Cation-specific interactions with carboxylate in amino acid and acetate aqueous solutions: x-ray absorption and ab initio calculations, *J. Phys. Chem. B* 112 (2008) 12567–12570.
- [44] I. Kalcher, D. Horinek, R.R. Netz, J. Dzubiella, Ion specific correlations in bulk and biointerfaces, *J. Phys. Condens. Matter* 21 (2009) 424108.
- [45] J.E. Shaw, R.F. Epand, K. Sinnathamby, Z. Li, R. Bittman, C.M. Yip, Tracking peptide-membrane interactions: insights from *in situ* coupled confocal-atomic force microscopy imaging of NAP-22 peptide insertion and assembly, *J. Struct. Biol.* 155 (2006) 458–469.
- [46] A. Mecke, D.-K. Lee, A. Ramamoorthy, B.G. Orr, M.M.B. Holl, Membrane thinning due to antimicrobial peptide binding: an atomic force microscopy study of MSI-78 in lipid bilayers, *Biophys. J.* 89 (2005) 4043–4050.
- [47] H.X. You, X. Qi, G.A. Grabowski, L. Yu, Phospholipid membrane interactions of saposin C: *in situ* atomic force microscopy study, *Biophys. J.* 84 (2003) 2043–2057.
- [48] W.-C. Huang, F.Y. Chen, C.-C. Lee, Y. Sun, M.-T. Lee, H.W. Huang, Membrane-thinning effect of curcumin, *Biophys. J.* 94 (2008) 4331–4338.
- [49] H.W. Huang, Deformation free energy of bilayer membrane and its effect on gramicidin channel lifetime, *Biophys. J.* 50 (1986) 1061–1070.
- [50] S. Ludtke, K. He, H.W. Huang, Membrane thinning caused by maganin 2, *Biochemistry* 34 (1995) 16764–16769.

- [51] H.A. Rinia, B. de Kruiff, Imaging domains in model membranes with atomic force microscopy, *FEBS Lett.* 504 (2001) 194–199.
- [52] A.J. Mason, M. Arnaud, B. Burkhard, Zwitterionic phospholipids and sterols modulate antimicrobial peptide-induced membrane destabilization, *Biophys. J.* 93 (2007) 4289–4299.
- [53] E.J. Prenner, R.A.N. Lewis, M. Jelokhani-Niaraki, R.S. Hodges, R.N. McElhaney, Cholesterol attenuates the interaction of the antimicrobial peptide gramicidin S with phospholipid bilayer membranes, *Biochim. Biophys. Acta* 1510 (2001) 83–92.
- [54] F. Nicol, S. Nir, F.C. Szoka Jr., Effect of cholesterol and charge on pore formation in bilayer vesicles by a pH-sensitive peptide, *Biophys. J.* 71 (1996) 3288–3301.
- [55] M.A. Churchward, T. Rogasevskaia, D.M. Brandman, H. Khosravani, P. Nava, J.K. Atkinson, J.R. Coorsen, Specific lipids supply critical negative spontaneous curvature—an essential component of native Ca²⁺-triggered membrane fusion, *Biophys. J.* 94 (2008) 3976–3986.
- [56] S.-A. Lee, Y.K. Kim, S.S. Lim, W.L. Zhu, W. Ko, S.Y. Shin, K.-S. Hahm, Y. Kim, Solution structure and cell selectivity of piscidin 1 and its analogues, *Biochemistry* 46 (2007) 3653–3663.